DOI: 10.13009/EUCASS2022-7363
9TH EUROPEAN CONFERENCE FOR AERONAUTICS AND SPACE SCIENCES (EUCASS)

Solid Rocket Motor Internal Ballistics Simulation Using Eulerian Multiphase Models

M. Grossi[⋆†]*, G. Cocirla*[⋆]*, D. Bianchi*[⋆] *and B. Favini*[⋆]
[⋆]*Dept. of Mechanical and Aerospace Engineering - Sapienza University of Rome*
Via Eudossiana 18, 00184 - Rome, Italy
marco.grossi@uniroma1.it · cocirla.1748383@studenti.uniroma1.it · daniele.bianchi@uniroma1.it · bernardo.favini@uniroma1.it
[†]Corresponding author

Abstract

Solid rocket motors, fuelled by aluminum, are characterized by a two-phase flow that plays an essential role in several aspects of the motor behavior. In the present work, the dispersed phase is considered via an advanced Eulerian model that exploits a pseudo-pressure term deprived of any calibration need in order to overcome the intrinsic limitations of the basic Eulerian monokinetic closure. Numerical simulations performed on different geometries and setups show promising results, ensuring the possibility to investigate solid rocket motors flowfield with relatively low computational costs.

1. Introduction

Multiphase flows constituted of liquid droplets or solid particles carried by a gaseous phase play a major role in a wide variety of industrial and scientific applications. Among the space propulsion technologies, modern Solid Rocket Motors (SRMs) are a clear example of such kind of flows. Current propellants are laden with metal particles, mainly aluminum, that compose up to the 20% of the total mass. The primary reason for the inclusion of such fuel particles into the solid propellant stems from the significant heat release obtained as the aluminum particles react to form aluminum oxides (Al_2O_3). As the propellant burns, the grain surface regresses and the particles added to the propellant melt to form liquid droplets. A complex mechanism follows, resulting in the release of aluminum agglomerates and their injection into the accelerating core flow [18]. The final size of the aluminum oxide particles is found to vary from a few micrometers to a few hundred micrometers, providing a polydisperse multiphase flow. Collisions between particles and breakup events near the motor nozzle generate further modification of particles distribution, exacerbating the already complex flowfield. Despite of its favourable effect on specific impulse, inclusion of *Al* particles in the propellant has some side effects. Indeed, it may lead to slag accumulation in submerged nozzles, thermoacoustic instability due to distributed combustion and, moreover, the alumina droplets are the main source of nozzle scouring from particulate impact, contributing to nozzle erosion. Two-phase flow losses in the nozzle expansion process caused by the velocity- and thermal-lag are also hindering the performance enhancement due to particle addition [21, 23]. For such reasons, a correct evaluation of such two-phase flowfield plays an important role in the study of this kind of propulsive systems.

SRM flows can hardly be investigated via experiments due to the severe internal conditions characterized by high temperatures and pressures. Therefore, numerical simulations are often mandatory to understand the underlying driving physics of the internal flow. To model the behaviour of alumina particles and their impact on the motor system, a wide variety of solutions have been proposed over the years and can be classified into two main categories, the Lagrangian and the Eulerian models. Lagrangian mathematical models, tracking each particle within the flow, are intrinsically able to represent in a very reliable way all the characteristic aspects of multiphase flows but, given the huge number of particles within SRMs, present large computational costs. Eulerian models, instead, solve the condensed phase in the same fixed reference frame of the gaseous carrier, offering relevant savings in terms of computational time. Eulerian descriptions are well suited for low inertia particles for which particles trajectory crossings do not occur. On the contrary, when the dispersed phase is characterized by larger inertia and particles trajectories should cross, Eulerian models are affected by the formation of a numerical, non-physical, particle dense structure called δ-shock [5]. The presence of δ-shocks leads to an incorrect evaluation of the coupling source terms and therefore to an inaccurate estimate of the flowfield.

In order to overcome the intrinsic limits of Eulerian methodologies, a wide range of mathematical closures have been developed. The first and most elementary models are based on a multi-family approach where the family selection

DOI: 10.13009/EUCASS2022-7363

criteria is about the velocity direction [3, 14, 19]. The selling point of such methodology is the possibility to completely avoid δ-shocks formation solving in a separate way the crossing particles jets. Despite the good results that this method allows to achieve, a multi-family framework is limited by the need of an a priori knowledge of the flowfield. Most advanced Eulerian models are built on a statistical approach based on the velocity moments equation arising from the integration of the Williams-Boltzmann Equation (WBE). The WBE conveniently describes all the characteristics of a condensed phase with numerous degrees of freedom, as size, velocity, and temperature. The moments governing equations, i.e. the set of conservation laws used to the describe the flowfield dynamics, are obtained integrating the WBE. Based on the closure strategy necessary to compute the fluxes terms, mathematical models may be distinguished into Algebraic Based Closure Moment Methods (ABCMM) [22, 12, 8] and Kinetic Based Closure Momment Methods (KBCMM) [15, 7, 11, 27, 2].

The aim of this work is the application of an advanced Eulerian formulation to solve the internal flows typical of SRMs. In particular, a comparison between different strategies is presented in order to show the improvement that can be achieved with enhanced modeling.

2. Two-Phase Modeling

The model employed in this work is based on a multidimensional formulation applied to a set of equations able to solve gaseous and condensed phases behaviour within motor chambers. The inviscid Euler set of equations are solved to describe the gaseous phase. As for the particles one, a fully Eulerian model is exploited, with condensed phase supposed dilute ($\frac{\rho_p}{\rho_{Al2O3}} \ll 1$) and assumed to be spherical. In the present model, a multifamily approach is followed: the overall condensed phase is decomposed in a certain number of particles groups, each one with its own set of equations. As the flow is dilute, only gas-particles interactions count whereas any coupling among the particles groups are neglected.

The general governing equations in compact form read:

$$\frac{\partial}{\partial t}\begin{pmatrix} W_g \\ W_{p,k} \end{pmatrix} + \nabla \cdot \begin{pmatrix} F_g \\ F_{p,k} \end{pmatrix} = \begin{pmatrix} S_g \\ S_{p,k} \end{pmatrix} \qquad , \qquad k = 1, \dots, N_k \tag{1}$$

where W denotes the conservative variable vector, F is the flux vector, and S is the two-way source term vector. Subscripts g and p stand respectively for the gaseous carrier phase and the condensed one. The subscript k identifies a single group of particles.

A full two-way coupling is enforced between the gaseous carrier and the groups of particles. In the present work both drag force and heat exchange are modelled accordingly with the work of Carlson and Hoglund [1], Miller [17] and, Shimada and Daimon [21]. For what concerns the drag force, the classical law for a cloud of n_p particles is employed:

$$\vec{F}_d = \frac{1}{8}\pi\rho_g d_p^2 n_p C_d (\vec{V}_g - \vec{V}_p)\|\vec{V}_g - \vec{V}_p\| \tag{2}$$

Where d_p is the particle diameter, n_p the number of particles per unit volume and C_d the drag coefficient, evaluated accordingly with the formulation derived by Henderson [9].
For $M_p \leq 1$.

$$\begin{aligned} C_d = 24 \Bigg[Re_p + M_p \left(\frac{\gamma}{2}\right)^{1/2} \Bigg[4.33 + \left(\frac{3.65 - 1.53\frac{T_p}{T_g}}{1 + 0.353\frac{T_p}{T_g}} \right) exp\left(-0.247 \frac{Re_p}{M_p\left(\frac{\gamma}{2}\right)^{1/2}} \right) \Bigg] \Bigg]^{-1} \\ + exp\left(-\frac{0.5 M_p}{Re_p^{1/2}} \right) \left[\frac{4.5 + 0.38(0.03 Re_p + 0.48 Re_p^{1/2})}{1 + 0.03 Re_p + 0.48 Re_p^{1/2}} + 0.1 M_p^2 + 0.2 M_p^8 \right] \\ + 0.6 M_p \left(\frac{\gamma}{2}\right)^{1/2} \left[1 - exp\left(-\frac{M_p}{Re_p} \right) \right] \end{aligned} \tag{3}$$

For $M_p \geq 1.75$.

$$C_d = \frac{0.9 + \frac{0.34}{M_p^2} + 1.86\left(\frac{M_p}{Re_p}\right)^{1/2} \left[2 + \frac{2}{M_p^2 \frac{\gamma}{2}} + \frac{1.058}{M_p\left(\frac{\gamma}{2}\right)^{1/2}} \right] \left(\frac{T_p}{T_g}\right)^{1/2} - \frac{1}{M_p^4 \frac{\gamma^2}{4}}}{1 + 1.86\left(\frac{M_p}{Re_p}\right)^{1/2}} \tag{4}$$

DOI: 10.13009/EUCASS2022-7363

Finally for the range $1 < M_p < 1.75$.

$$C_d = C_d(1.0, Re_p) + \frac{3}{4}(M_p - 1)[C_d(1.75, Re_p) - C_d(1.0, Re_p)] \tag{5}$$

where Re_p and M_p respectively represent the Particulate Reynolds and Mach numbers:

$$Re_p = \frac{\rho_g \|\vec{V}_g - \vec{V}_p\| \, d_p}{\mu_g} \tag{6}$$

$$M_p = \frac{\|\vec{V}_g - \vec{V}_p\|}{a} \tag{7}$$

Assuming that radiation is actually negligible, convection is the sole heat exchange phenomenon taken into account. Its relation reads:

$$Q_c = \pi \frac{\lambda_g}{\mu_g} d_p^2 n_p (T_g - T_p) Nu \tag{8}$$

where λ_g is the gaseous thermal conductivity, μ_g is dynamic viscosity. Finally, the Nusselt number Nu is evaluated through the well-known Kavanau-Drake [13] correction:

$$Nu = \frac{2 + 0.458 Re_p^{0.55} Pr^{0.33}}{1 + 3.42 \frac{M_p}{Re_p Pr}(2 + 0.459 Re_p^{0.55} Pr^{0.33})} \tag{9}$$

2.1 Monokinetic Model - MK

The Monokinetic (MK) approach represents the basic pressure-less closure of Eulerian descriptions [16]. It assumes that for a given position and time, all particles have the same velocity, a conditions that naturally leads to the generation of $\delta-$shocks. The corresponding terms of Eq.1 valid for the MK are reported in Eq.10:

$$W_P = \begin{pmatrix} \rho_p \\ \rho_p \vec{V}_p \\ \rho_p e_p \end{pmatrix} \qquad F_p = \begin{pmatrix} \rho_p \vec{V}_p \\ \rho_p \vec{V}_p \otimes \vec{V}_p \\ \rho_p \vec{V}_p e_p \end{pmatrix} \qquad S_p = \begin{pmatrix} 0 \\ \vec{F}_d \\ \vec{F}_d \cdot \vec{V}_p + Q_c \end{pmatrix} \tag{10}$$

The total energy of the dispersed phase e_P is the sum of thermal and kinetic energy. In the MK model has the following expression:

$$\rho_p e_p = \rho_p c_{Al_2O_3} T_p + \frac{1}{2} \rho_p \|\vec{V}_p\|^2 \tag{11}$$

where $c_{Al_2O_3}$ is the thermal capacity of alumina and T_p is the particle temperature.

2.2 Isotropic Gaussian Model

In order to deal with high inertia particles, the polykinetic aspect of the multiphase flow has to be taken into account. The approach chosen in the present work assumes the moment equations up to the second order, enabling to consider not only the average velocity value but also a local velocity dispersion. The Isotropic Gaussian (IG) approach, derived by Levermore and Morokoff [15], is able to retain the existence of different crossing particle trajectories through the generation of an isotropic pseudo-pressure term P_p, proportional to the particle density. It is convenient to define $\underline{P}$ as a diagonal matrix of size equal to the spatial dimension of the addressed problem with elements equal to P_p. The IG governing equations read:

DOI: 10.13009/EUCASS2022-7363

$$W_p = \begin{pmatrix} \rho_p \\ \rho_p \vec{V}_p \\ \rho_p e_{kin} \\ \rho_p e_p \end{pmatrix} \qquad F_p = \begin{pmatrix} \rho_p \vec{V}_p \\ \rho_p \vec{V}_p \otimes \vec{V}_p + \underline{P} \\ (\rho_p e_{kin} + P_p)\vec{V}_p \\ (\rho_p e_p + P_p)\vec{V}_p \end{pmatrix} \qquad S_p = \begin{pmatrix} 0 \\ \vec{F}_d \\ \vec{F}_d \cdot \vec{V}_p + 3P_p/\tau_p \\ \vec{F}_d \cdot \vec{V}_p + 3P_p/\tau_p + Q_c \end{pmatrix} \tag{12}$$

Where τ_p is the characteristic kinetic relaxation time of the dispersed phase related to the particle diameter and used drag model correction as shown in Eq.13 [26].

$$\tau_p = \frac{\rho_p d_p^2}{18\mu_g} \frac{24}{C_d Re_p} \tag{13}$$

The variable e_{kin} is the turbulent kinetic energy that is linked to the pseudo-pressure term by the following equation:

$$\rho_p e_{kin} = \frac{1}{2}\rho_p \|\vec{V}_p\|^2 + \frac{3}{2}P_p \tag{14}$$

The total energy e_p remains the sum of the thermal and kinetic contribution, the latter now including also the turbulent part.

$$\rho_p e_p = \rho_p c_{Al_2O_3} T_p + \rho_p e_{kin} \tag{15}$$

The introduced pseudo-pressure term alters both momentum and energy conservation laws, generating a motion of the dispersed phase from high to low particles concentration regions, allowing to break δ-shocks and thus obtaining a better representation of the SRM flow field. It is worth to note that the model does not need any calibration term.

3. Numerical Results

In order to highlight the advantages and limitations of the aforementioned mathematical models, two numerical test simulations, with increasing complexity, have been carried out. The presented computations have been provided by the DIMA in-house code based on a finite volume Godunov numerical scheme [10] and multi-blocks structured meshing. Conservative variables are calculated at the center of each computational cell whereas convective fluxes are computed at cell interfaces using an approximate Roe Riemann Solver [24] for the gaseous phase, a Saurel Particulate Solver [20] for the MK closure and an HLL Riemann Solver [24, 5, 6] with the simple speed wave evaluation algorithm by Davis [4] for the IG closure. Space discretization is performed thanks to a second order TVD scheme in which the interface reconstruction strategy proposed by Doisneau [5] and Vié [25] was followed in order to ensure that moments did not lose their physical meaning (negative density or pressure are not allowed), while second order accuracy in time is recovered using an explicit two-steps Runge-Kutta approach.

3.1 JAXA Planar Nozzle

The first test case under analysis consists in a mono-disperse multiphase flow due to the injection of particles into the divergent section of a planar nozzle [21]. The injectors are located on the lower and upper walls downstream the throat, resulting in a symmetrical configuration, as it is possible to see in Fig.1. The physical features regarding boundary conditions for gas and particles may be found in Ref.[21].

CFD simulations are performed with three different model closures: MK with $N_k = 1$ (MK-1), MK with $N_k = 2$ (MK-2), and IG. For what concerns the second set-up, the MK-2, each group is injected from a single wall. Numerical outcomes regarding the particle density field for the three closures are shown and compared in Fig.2 along with a Lagrangian solution extracted from the reference work.

In the MK-1 result, visible in Fig.2a, the formation of a δ-shock along the symmetry axis is clearly evident. This behaviour is due to the presence of a single averaged value of the dispersed phase velocity in each cell. As a matter of fact, when the two particles jets cross, the vertical momentum component is cancelled out and only the axial component remains. Comparing the solution obtained with the MK-1 approach with the Lagrangian envelope (green lines in Fig.2a), it can be deduced that the presence of particles crossings makes the MK model unrepresentative of the physical reality and therefore not particularly suitable for this type of applications. The intrinsic limitations of the

DOI: 10.13009/EUCASS2022-7363

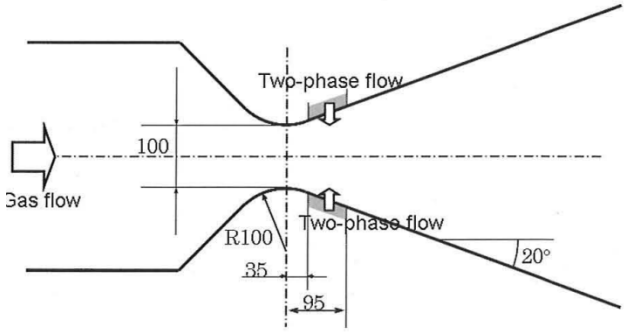

Figure 1: JAXA planar nozzle geometry [21].

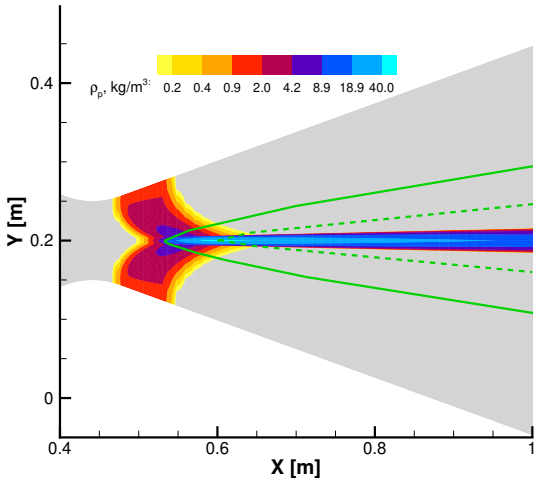

(a) MK closure, $N_k = 1$

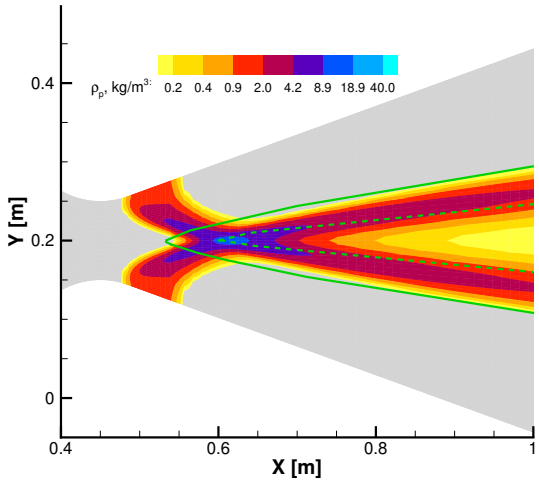

(b) MK closure, $N_k = 2$.

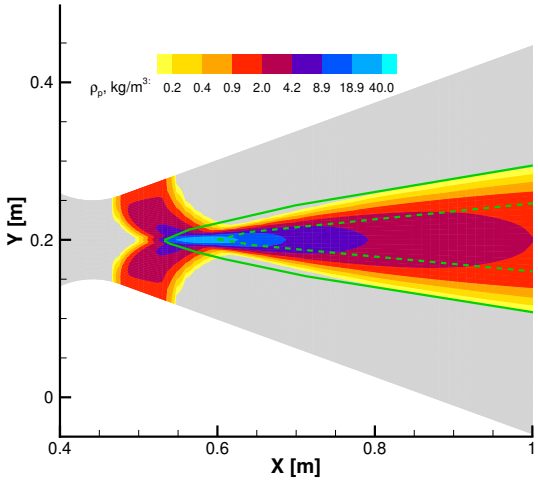

(c) IG closure.

Figure 2: Particles density field for the JAXA planar nozzle (green lines identify the Lagrangian solution).

MK closure may be effectively overcome thanks to a multi-family approach. In fact, addressing the solution proposed in Fig.2b, it is evident that by defining two particles families, one for each injection location, it is possible to obtain

DOI: 10.13009/EUCASS2022-7363

a flowfield solution much more similar to the Lagrangian one: the two jets cross without interacting, avoiding the formation of any $\delta-$shock, so to generate an emptier region downstream of the crossing point. Of course, the enhanced quality of this outcomes is paid with heavier computational loads since two separate sets of equations, one for each particles group, must be solved on the entire grid. Finally, the IG result is presented in Fig.2c. Contrary to the MK-1, the δ-shock structure is broken and the particles are dispersed in all directions, following the isotropic nature of the mathematical closure. Comparing this solution with the Lagrangian reference one, a good agreement is actually achieved just adding only one more equation with regard to the MK-1 closure.

3.2 Aft-Finocyl Solid Rocket Motor

A more complex test case is hereafter presented. It consists in an axisymmetric aft-finocyl SRM geometry featured in Fig.3. An injection boundary condition is applied to the solid propellant surface, providing mass and energy flowrates for both gaseous and condensed phases. Unlike the previous simulations, the typical polydisperse aspect of SRMs flows is taken into account considering both alumina smoke ($d_p = 2\,\mu m$) and large oxide droplets ($d_p = 100\,\mu m$). CFD simulations are performed applying several model closure: MK-1, MK-5 and IG. Note that the number in these acronyms identifies only the amount of groups associated to large alumina particles. A further group is injected in each simulation to account for the alumina smoke. Regarding the MK-5, the several families associated to large particles are separately injected from the propellant surface at every major slope change of the geometry.

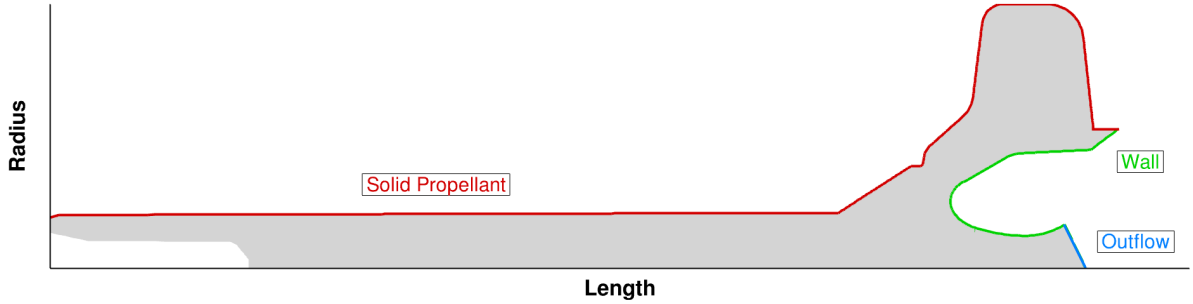

Figure 3: Aft-finocyl SRM geometry.

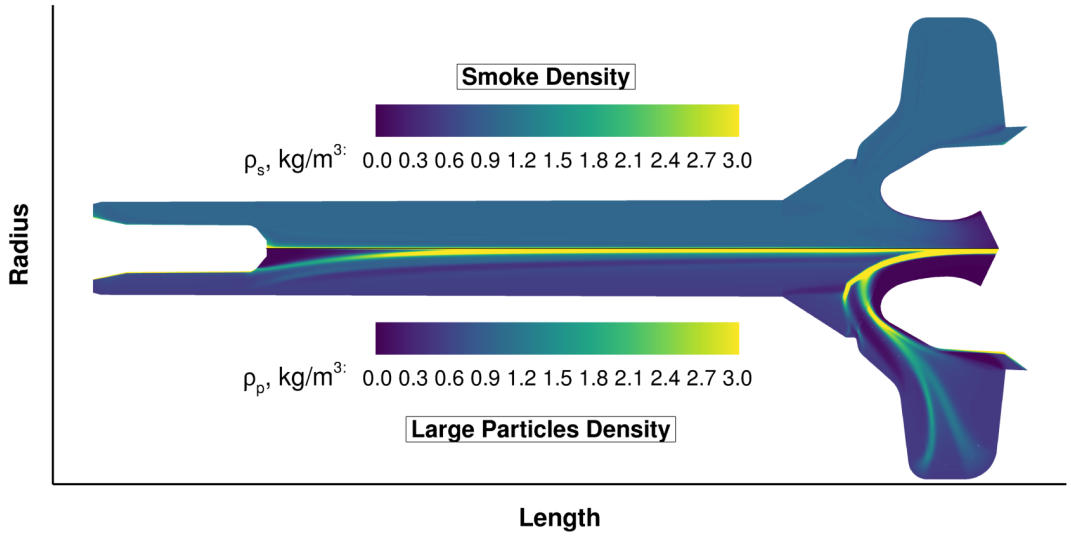

Figure 4: MK-1 solution for the aft-finocyl SRM.

In Fig.4, the MK-1 particles density field is shown for both large and small particles. As it is possible to see, the smoke density presents a very homogeneous behaviour, typical of low inertia droplets, whereas the large particles flowfield is characterized by the presence of relevant accumulations, with density values peaking at nearly $500\,kg/m^3$,

DOI: 10.13009/EUCASS2022-7363

a really high value that compromises the hypothesis of dilute two-phase flow. Contrary to what has been presented for the JAXA planar nozzle, a greater number of particles groups do not alleviate the scenario. Indeed, as it is evident in Fig.5, the two flowfields concerning MK-1 and MK-5 are very similar, with minor differences in the region close to the nozzle.

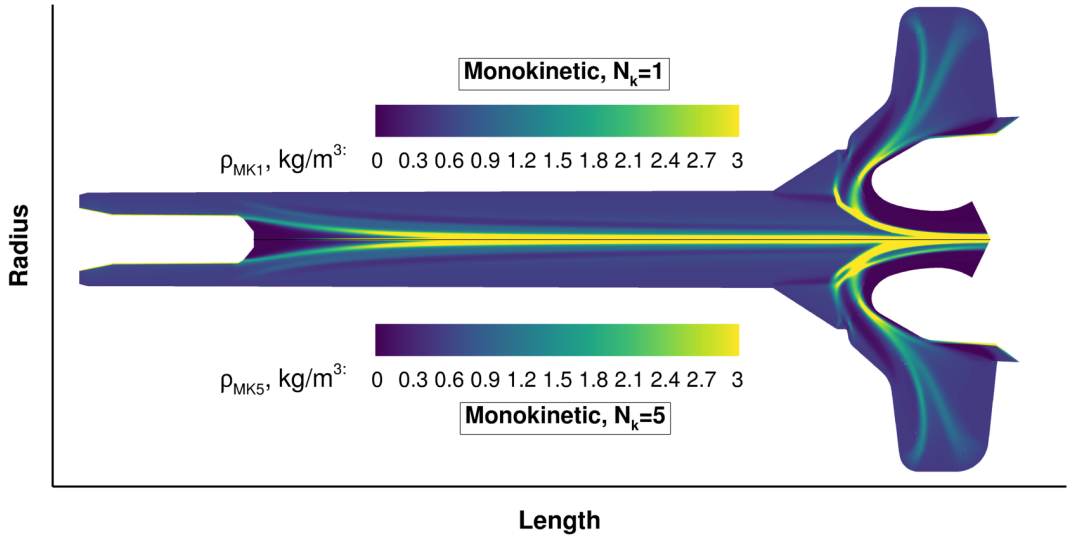

Figure 5: MK-1 vs MK-5 solutions for the aft-finocyl SRM.

Finally, results concerning the application of the IG closure are presented in Fig.6. Both particles density and pseudo-pressure flowfields are reported in order to give major insights in the model functioning. Looking at the density flowfield, a solution very similar to the one already seen for the MK is obtained. The pseudo-pressure closely follows the density field, showing higher values where the particles tend to accumulate.

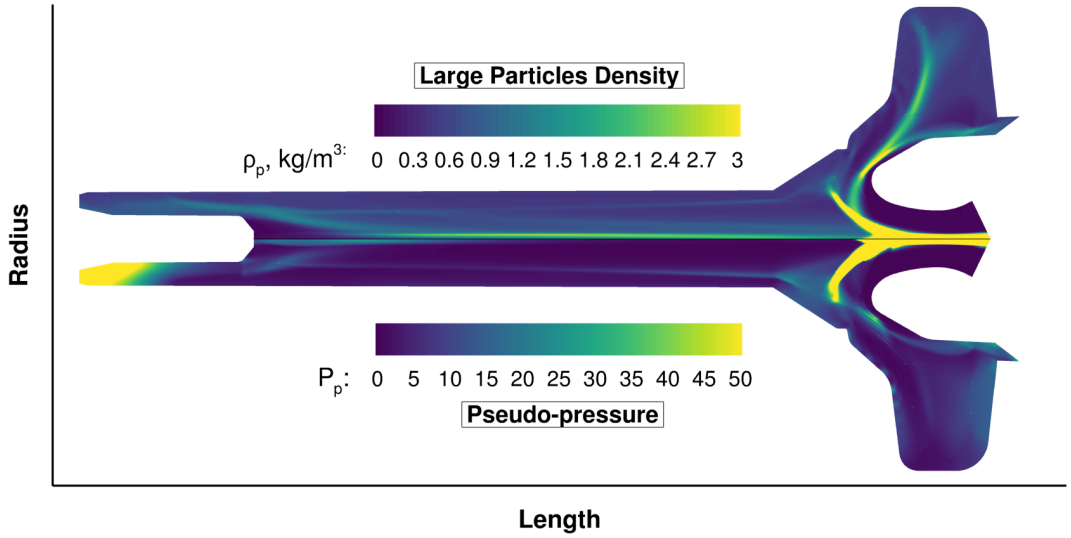

Figure 6: IG solution for the aft-fynocil SRM.

However, an important improvement is actually achieved thanks to the IG closure. The pseudo-pressure term enables a redistribution of the particles, strongly reducing the accumulates. This behaviour is clearly witnessed by Fig.7 that represents the particle density profile along the motor radius for a certain longitudinal position for the two

DOI: 10.13009/EUCASS2022-7363

different closures. As it is possible to see, the density peak is decidedly lower for the IG, assuring the validity of the modeling assumptions.

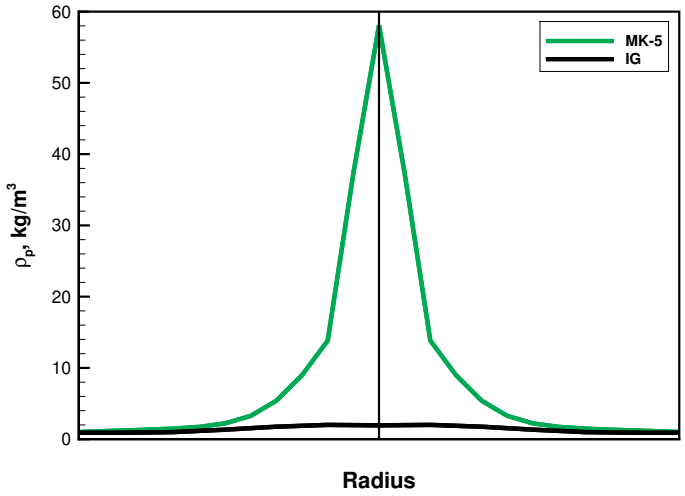

Figure 7: MK vs IG results for particles density profile.

4. Conclusions

Current Solid Rocket Motors (SRM) employed in the space transportation system are characterized by a two-phase flow that needs to be correctly evaluated in order to investigate the internal flow dynamics. As the basic monokinetic Eulerian model presents important drawbacks (non-physical accumulation of particles), statistical approaches in the kinetic theory framework are nowadays preferred. In the present work, a particular Eulerian closure model, named Isotropic Gaussian, is considered. The applied method accounts for the effect of the local particle distribution, via a pseudo-pressure term with no need for any calibration. Two test cases have been analyzed: a simple planar nozzle and an aft-finocyl SRM. Both simulations have emphasized the good ability of the IG closure to capture particle dynamics and dispersion and have highlighted the model potential to keep true the dilute flow hypothesis even in presence of a flowfield characterized by large inertia particles.

References

[1] Donald J Carlson and Richard F Hoglund. Particle drag and heat transfer in rocket nozzles. *Aiaa Journal*, 2(11):1980–1984, 1964.

[2] Christophe Chalons, Rodney O Fox, Frédérique Laurent, Marc Massot, and Aymeric Vié. Multivariate gaussian extended quadrature method of moments for turbulent disperse multiphase flow. *Multiscale Modeling & Simulation*, 15(4):1553–1583, 2017.

[3] E Daniel, R Saurel, M Larini, and JC Loraud. A multiphase formulation for two phase flows. *International Journal of Numerical Methods for Heat & Fluid Flow*, 1994.

[4] SF Davis. Simplified second-order godunov-type methods. *SIAM Journal on Scientific and Statistical Computing*, 9(3):445–473, 1988.

[5] François Doisneau. *Eulerian modeling and simulation of polydisperse moderately dense coalescing spray flows with nanometric-to-inertial droplets: application to Solid Rocket Motors*. PhD thesis, Ecole Centrale Paris, 2013.

[6] Valentin Dupif. *Eulerian modeling and simulation of two-phase flows in solid rocket motors taking into account size polydispersion and droplet trajectory crossing*. PhD thesis, Université Paris Saclay (COmUE), 2018.

[7] Rodney O. Fox. A quadrature-based third-order moment method for dilute gas-particle flows. *Journal of Computational Physics*, 227(12):6313–6350, 2008.

DOI: 10.13009/EUCASS2022-7363

[8] Sarah Hank, Richard Saurel, and Olivier Le Metayer. A hyperbolic eulerian model for dilute two-phase suspensions. *Journal of Modern Physics*, 2011, 2011.

[9] Charles B Henderson. Drag coefficients of spheres in continuum and rarefied flows. *AIAA journal*, 14(6):707–708, 1976.

[10] Charles Hirsch. *Numerical computation of internal and external flows: The fundamentals of computational fluid dynamics*. Elsevier, 2007.

[11] Damien Kah, Frédérique Laurent, Lucie Fréret, Stephane De Chaisemartin, Rodney O Fox, Julien Reveillon, and Marc Massot. Eulerian quadrature-based moment models for dilute polydisperse evaporating sprays. *Flow, Turbulence and Combustion*, 85(3):649–676, 2010.

[12] A Kaufmann, Mathieu Moreau, Olivier Simonin, and Jérôme Helie. Comparison between lagrangian and mesoscopic eulerian modelling approaches for inertial particles suspended in decaying isotropic turbulence. *Journal of Computational Physics*, 227(13):6448–6472, 2008.

[13] Lawrence Lewis Kavanau and RM Drake Jr. Heat transfer from spheres to a rarefied gas in subsonic flow. Technical report, CALIFORNIA UNIV BERKELEY INST OF ENGINEERING RESEARCH, 1953.

[14] Frédérique Laurent and Marc Massot. Multi-fluid modelling of laminar polydisperse spray flames: origin, assumptions and comparison of sectional and sampling methods. *Combustion theory and modelling*, 5(4):537, 2001.

[15] C. David Levermore and William J. Morokoff. The gaussian moment closure for gas dynamics. *SIAM Journal on Applied Mathematics*, 59(1):72–96, 1998.

[16] Frank E Marble. Dynamics of dusty gases. *Annual Review of Fluid Mechanics*, 2:397–446, 1970.

[17] William H Miller. *Solid rocket motor performance analysis and prediction*, volume 8039. National Aeronautics and Space Administration, 1971.

[18] E.W Price and R.K. Sigman. Combustion of aluminized solid propellants. *Solid propellant chemistry, combustion, and motor interior ballistics*, 185:663–687, 2000.

[19] JS Sachdev, CPT Groth, and JJ Gottlieb. Numerical solution scheme for inert, disperse, and dilute gas-particle flows. *International journal of multiphase flow*, 33(3):282–299, 2007.

[20] Richard Saurel, Eric Daniel, and Jean Claude Loraud. Two-phase flows-second-order schemes and boundary conditions. *AIAA journal*, 32(6):1214–1221, 1994.

[21] Toru Shimada, Yu Daimon, and Nobuhiro Sekino. Computational fluid dynamics of multiphase flows in solid rocket motors. Technical report, Japan Aerospace Exploration Agency (JAXA), 2006.

[22] Marine Simoes, Patrick Della Pieta, Franck Godfroy, and Olivier Simonin. Continuum modeling of the dispersed phase in solid rocket motors. In *17th AIAA Computational Fluid Dynamics Conference*, page 4698, 2005.

[23] Piyush Thakre, Rajesh Rawat, Richard Clayton, and Vigor Yang. Mechanical erosion of graphite nozzle in solid-propellant rocket motor. *Journal of Propulsion and Power*, 29(3):593–601, 2013.

[24] Eleuterio F Toro. *Riemann solvers and numerical methods for fluid dynamics: a practical introduction*. Springer Science & Business Media, 2013.

[25] Aymeric Vié, François Doisneau, and Marc Massot. On the anisotropic gaussian velocity closure for inertial-particle laden flows. *Communications in Computational Physics*, 17(1):1–46, 2015.

[26] Junlong Wang, Ningfei Wang, Xiangrui Zou, Wei Dong, Chao Wang, Lei Han, and Baolu Shi. Experimental and numerical study on slag deposition in solid rocket motor. *Aerospace Science and Technology*, 122:107404, 2022.

[27] Cansheng Yuan and Rodney O Fox. Conditional quadrature method of moments for kinetic equations. *Journal of Computational Physics*, 230(22):8216–8246, 2011.